Supplementary Notes

Spine Ca^{2+} signals produced by glutamate uncaging

We imaged uncaging-evoked [Ca^{2+}] transients in neurons loaded with a green Ca^{2+}-sensitive indicator (G; 500 μM Fluo 4FF) and a red Ca^{2+}-insensitive dye (R; 30 μM Alexa 594) (Supplementary Fig 1a). To calculate [Ca^{2+}] from fluorescence measurements, we used the relationship:

$$\frac{G/R}{(G/R)_{\max}} = \frac{[Ca^{2+}]}{K_D + [Ca^{2+}]}$$

where $(G/R)_{max}$ is the green-to-red fluorescence ratio at saturating [Ca^{2+}] and the dissociation constant, K_D, of Fluo 4FF is 10.4 μM[1].

The presence of Ca^{2+}-sensitive indicators increases the cytoplasmic buffer capacity (κ) and decreases the amplitudes of [Ca^{2+}] transients ($\Delta[Ca^{2+}]$)[1]. The endogenous buffer capacity (κ_E) for hippocampal spines is ~ 20[(2)]. The added buffer capacity due to the presence of [Ca^{2+}] indicator (κ_{dye}) can be calculated as:

$$\kappa_{dye} = \frac{K_D[B]_{total}}{(K_D + [Ca^{2+}])^2} \quad \text{(Ref 1)}$$

where $[B]_{total}$ is the total buffer concentration. Therefore 500 μM Fluo 4FF adds a buffer capacity of $\kappa_{dye} \sim 50$.

NMDA receptor-mediated [Ca^{2+}] accumulations can be described as:

$$\Delta[Ca^{2+}] = \frac{Q\beta^{-1}}{V_{sp}(1-\Gamma\beta^{-1}\tau_{NMDA})}\left[\exp\left(-\frac{\Gamma t}{\beta}\right) - \exp\left(-\frac{t}{\tau_{NMDA}}\right)\right] \quad \text{(Ref 1)}$$

where Q is the total amount (moles) of Ca^{2+} influx, V_{sp} is the volume of the spine, Γ is the extrusion rate constant (1600 s^{-1} [(2)]), τ_{NMDA} is the decay time constant of the NMDA receptor-mediated current (~ 100 ms; Supplementary Fig. 1a), and $\beta = (1 + \kappa_E + \kappa_{dye})$. The time of peak [$Ca^{2+}$] accumulation, t_{peak}, can be calculated as:

$$t_{peak} = \frac{\ln\left(\frac{\beta}{\Gamma\tau_{NMDA}}\right)}{-\frac{\Gamma}{\beta} + \frac{1}{\tau_{NMDA}}}$$

Therefore, peak $[Ca^{2+}]$ accumulations are expected to be reduced by a factor of ~ 1.4 due to the presence of the Ca^{2+} indicator.

Peak uncaging-evoked $[Ca^{2+}]$ accumulations during the LTP protocol in low extracellular Mg^{2+} and 4 mM extracellular Ca^{2+} were ~ 3.3 μM (Supplementary Fig 1c), corresponding to ~ 4.6 μM in the absence of indicator. This value is smaller than the Ca^{2+} concentrations measured during low-frequency synaptic stimulation at 0 mV[(2)] and is therefore in a physiological range. During the subthreshold protocol, peak $[Ca^{2+}]$ accumulations were ~ 0.7 μM (Supplementary Fig 1c), corresponding to ~ 1.0 μM in the absence of indicator.

At a postsynaptic potential of ~ 0 mV in 2 mM extracellular Ca^{2+} and 1 mM extracellular Mg^{2+}, peak $[Ca^{2+}]$ accumulations during the LTP protocol were ~ 1.8 μM (Supplementary Fig 1c), or ~ 2.5 μM without exogenous buffer. During the subthreshold protocol, peak $[Ca^{2+}]$ accumulations were ~ 0.3 μM (Supplementary Fig 1c), corresponding to ~ 0.4 μM in the absence of indicator.

Uncaging pulses did not produce detectable $[Ca^{2+}]$ accumulations in nearby spines (< 3 μm from the stimulated spine, mean distance = 1.7 ± 0.4 μm), either in low extracellular Mg^{2+} ($\Delta[Ca^{2+}]_{\text{nearby spine, LTP pulse}}$ = 0.03 ± 0.04 μM, $p > 0.6$; $\Delta[Ca^{2+}]_{\text{nearby spine, sub pulse}}$ = 0.02 ± 0.04 μM, $p > 0.7$) or at a postsynaptic potential of ~ 0 mV ($\Delta[Ca^{2+}]_{\text{nearby spine, LTP pulse}}$ = 0.02 ± 0.03 μM, $p > 0.6$; $\Delta[Ca^{2+}]_{\text{nearby spine, sub pulse}}$ = 0.01 ± 0.04 μM, $p > 0.9$) (Supplementary Fig 1c). These data show that uncaging-evoked $[Ca^{2+}]$ accumulations were restricted to the stimulated spine. Because $[Ca^{2+}]$ imaging can detect the activation of individual NMDA-Rs[3], these data further indicate that glutamate did not diffuse over intersynaptic distances to stimulate nearby spines. Finally, our $[Ca^{2+}]$ measurements were performed with high concentrations of exogenous buffer, which prolongs the time course and thus promotes the spatial spread of the $[Ca^{2+}]$ signal[2]. All plasticity experiments (Figs 1-6, Supplementary Fig 2) were performed without exogenous Ca^{2+} buffer and therefore will show even greater compartmentalization of Ca^{2+}.

Glutamate-independent effects of uncaging

Uncaging generates diffusible photoproducts in addition to glutamate, including protons that locally decrease the extracellular pH[4]. We tested if the uncaging process and its non-glutamate photoproducts contribute to crosstalk. We applied the LTP protocol (30 pulses at 0.5 Hz, 4 ms pulse duration; see Fig 1) at a single spine (LTP spine) at a postsynaptic potential of ~ -70 mV, preventing the induction of LTP. Ninety seconds later we applied the subthreshold protocol (30 pulses at 0.5 Hz, 1 ms pulse duration; see Fig1) at a nearby spine (sub spine), at ~ 0 mV. Under these conditions uEPSC amplitudes and spine volumes did not change at either spine ($\Delta uEPSC_{LTP\ spine}$ = -8 ± 6 %, $p > 0.3$; $\Delta uEPSC_{sub\ spine}$ = -6 ± 8 %, $p > 0.6$; $\Delta vol_{LTP\ spine}$ = -4 ± 5 %, $p > 0.5$; $\Delta vol_{sub\ spine}$ = 3 ± 7 %, $p > 0.7$). Non-glutamate photoproducts generated by uncaging therefore did not induce LTP, spine enlargement, or crosstalk. Also, LTP induction and spine enlargement required the pairing of uncaging and postsynaptic depolarization, supporting the involvement of NMDA-Rs (Fig 6b). Finally, these results argue that crosstalk is triggered by LTP induction.

Supplementary Methods

Preparation

Hippocampal slice cultures were prepared from postnatal day 6 or 7 rats[5], in accordance with the animal care and use guidelines of Cold Spring Harbor Laboratory and Janelia Farm Research Campus (Supplementary Fig 2). After 5-8 days in culture, cells were transfected by ballistic gene transfer using gold beads (~ 15 mg, 1.6 μm diameter) coated with 10 μg of plasmid DNA. Experiments were performed 2-3 days post-transfection. Imaging and glutamate uncaging were performed under the same conditions as with acute slices.

Controls for inhibitor function

To test the efficacy of thapsigargin and ryanodine (Supplementary Fig 3), a CA1 cell in an acute hippocampal slice was filled with 500 μM Fluo 4FF and 30 μM Alexa 594. Caffeine (40 mM in ACSF) was pressure applied for 2 seconds from a pipette located ~ 20 μm from the soma of the filled cell[6]. Caffeine-induced [Ca^{2+}] transients in

the soma were measured before and 5 minutes after the application of 1 μM thapsigargin and 20 μM ryanodine.

To test protein synthesis inhibitor function (Supplementary Fig 4), cells in cultured rat hippocampal slices were transfected with destabilized EGFP[7]. Slices were incubated in ACSF at room temperature. Changes in green fluorescence intensity in the thick apical dendrite were monitored following application of DMSO (0.1 %), 25 μM anisomycin, 60 μM cycloheximide, or 50 μM emetine.

Microscope design for two-photon imaging and glutamate uncaging

Two-photon imaging and glutamate uncaging were performed using a custom-built microscope with two Ti:sapphire lasers (MaiTai, Spectra Physics), as described[8]. Briefly, the intensity of each beam was controlled independently by electro-optical modulators (Pockels cells, Conoptics). Polarization angle was set using a half-wave plate. The beams were combined with a polarizing beam splitting cube (CVI Laser Optics) and passed through the same set of scan mirrors and objective (60x, 0.9 NA; Olympus). To aid alignment, two steering mirrors were used for each beam. The upstream position steering mirror (PSM) adjusted the position of the beam at the back focal plane of the objective. The downstream angle steering mirror (ASM) was placed in a conjugate plane to the scan mirrors and back focal plane of the objective using a Keplerian telescope consisting of two long focal length plano-convex lenses. Adjustment of the ASM changed the angle, but not the position, of the beam at the back focal plane of the objective, thus moving the beam in the sample plane. Coarse alignment was first performed to center the beams at the back focal plane of the objective. For fine alignment at the sample plane, 0.1 μm fluorescent beads were imaged simultaneously with both beams. The ASMs were adjusted until the images overlapped. The x, y, and z resolutions (full width at half maximum) for the imaging beam (910 nm) were 0.53 μm, 0.59 μm, and 1.89 μm, respectively. For the uncaging beam (720 nm), the x, y, and z resolutions (full width at half maximum) were 0.50 μm, 0.56 μm, and 1.66 μm, respectively.

Green and red fluorescence photons were separated using a dichroic mirror (565 nm) and bandpass filters (510/70, 635/90; Chroma). Photons were collected using photomultiplier tubes (PMTs; Hamamatsu R3896 except for the epifluorescence green

signal, Hamamatsu H7422-40). Epi- and transfluorescence signals were collected and summed[9].

References

1. Yasuda, R. et al. Imaging calcium concentration dynamics in small neuronal compartments. *Sci STKE* **2004**, pl5 (2004).
2. Sabatini, B.S., Oertner, T.G. & Svoboda, K. The life-cycle of Ca^{2+} ions in spines. *Neuron* **33**, 439-452 (2002).
3. Nimchinsky, E.A., Yasuda, R., Oertner, T.G. & Svoboda, K. The number of glutamate receptors opened by synaptic stimulation in single hippocampal spines. *J Neurosci* **24**, 2054-2064 (2004).
4. Canepari, M., Nelson, L., Papageorgiou, G., Corrie, J.E. & Ogden, D. Photochemical and pharmacological evaluation of 7-nitroindolinyl-and 4-methoxy-7-nitroindolinyl-amino acids as novel, fast caged neurotransmitters. *J Neurosci Methods* **112**, 29-42. (2001).
5. Stoppini, L., Buchs, P.A. & Muller, D.A. A simple method for organotypic cultures of nervous tissue. *J. Neurosci. Methods* **37**, 173-182 (1991).
6. Garaschuk, O., Yaari, Y. & Konnerth, A. Release and sequestration of calcium by ryanodine-sensitive stores in rat hippocampal neurones. *J. Physiol.* **502**, 13-30 (1997).
7. Li, X. et al. Generation of destabilized green fluorescent protein as a transcription reporter. *J Biol Chem* **273**, 34970-34975 (1998).
8. Pologruto, T.A. Doctoral thesis. Imaging neural activity and [Ca^{2+}] with genetically encoded calcium indicators and two-photon excitation laser scanning microscopy. (Harvard University, Cambridge, MA; 2004).
9. Mainen, Z.F. et al. Two-photon imaging in living brain slices. *Methods* **18**, 231-239 (1999).

Supplementary Figure 1

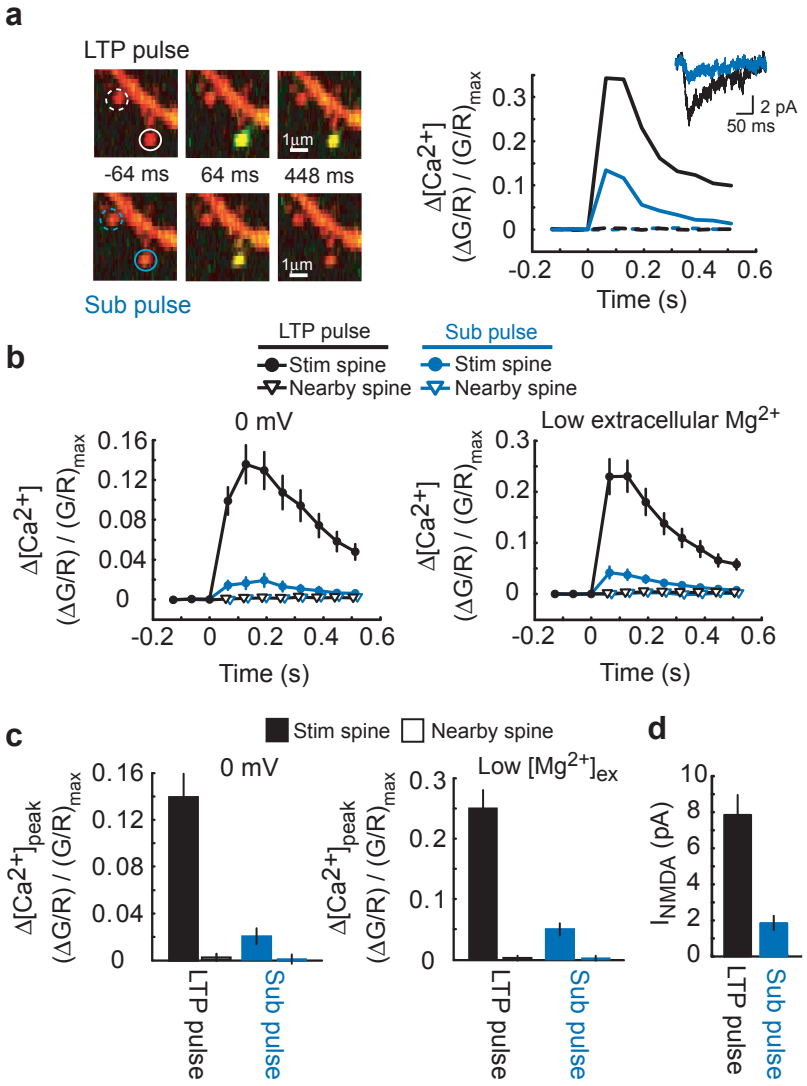

Supplementary Figure 1 | Characterization of glutamate uncaging pulses. a, Left panels, example $[Ca^{2+}]$ images for individual pulses from the LTP (4 ms pulse duration) and subthreshold (1 ms pulse duration) protocols in low extracellular Mg^{2+}. The cell was filled with a red Ca^{2+}-insensitive dye (R; 30 μM Alexa 594) and a green Ca^{2+}-sensitive dye (G; 500 μM Fluo 4FF). At time = 0, a single uncaging pulse was given at the spine marked by the solid circle. Right panels, time-course of uncaging-evoked $[Ca^{2+}]$ transients triggered by LTP pulses (black) and subthreshold pulses (blue) in the stimulated (solid line) and nearby spines (dashed line). Example NMDA-R currents (averaged over 5 trials) are shown. **b,** $[Ca^{2+}]$ transients in stimulated and nearby spines for LTP or subthreshold pulses at 0 mV (left; in 2 mM extracellular Ca^{2+} and 1 mM extracellular Mg^{2+}; n = 14 spines from 3 cells) and in low extracellular Mg^{2+} (right; at -70 mV in 4 mM extracellular Ca^{2+} and nominally 0 mM extracellular Mg^{2+}; n = 18 spines from 3 cells, mean ± sem). **c,** Peak $[Ca^{2+}]$ accumulations in stimulated and nearby spines for LTP and subthreshold pulses at 0 mV or in low extracellular Mg^{2+}. Data are from (b). **d,** NMDA-R currents for the LTP and subthreshold pulses in low extracellular Mg^{2+}. NBQX (10 μM) was added to isolated NMDA-R currents. n = 18 spines from 3 cells, mean ± sem.

Supplementary Figure 2

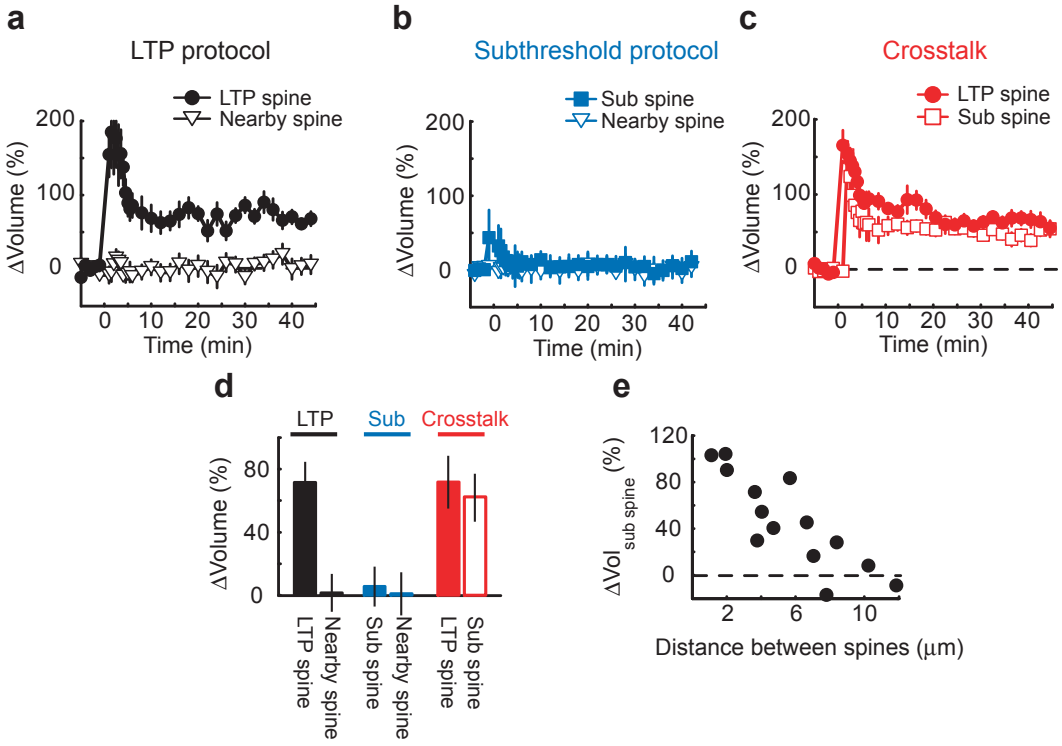

Supplementary Figure 2 | Crosstalk in cultured rat hippocampal slices. a, Time-course of the spine volume changes induced by the LTP protocol in GFP-expressing CA1 cells. At time = 0 the LTP protocol was applied to the LTP spine (in low extracellular Mg^{2+}). n = 6, mean ± sem. **b,** Time-course of the spine volume changes induced by the subthreshold protocol. At time = 0 the subthreshold protocol was applied to the sub spine (in low extracellular Mg^{2+}). n = 5, mean ± sem. **c,** Time-course of the spine volume changes for the crosstalk case. At time = 0 the LTP protocol was applied to the LTP spine and, 90 seconds later, the subthreshold protocol was given at a nearby spine (sub spine). n = 6, mean ± sem. **d,** Spine volume changes for the LTP protocol only, the subthreshold protocol only, and the crosstalk cases. Error bars indicate mean ± sem. **e,** Length scale of crosstalk. The LTP protocol was applied to the LTP spine and, 90 seconds later, the subthreshold protocol was applied to a neighboring spine (sub spine).

Supplementary Figure 3

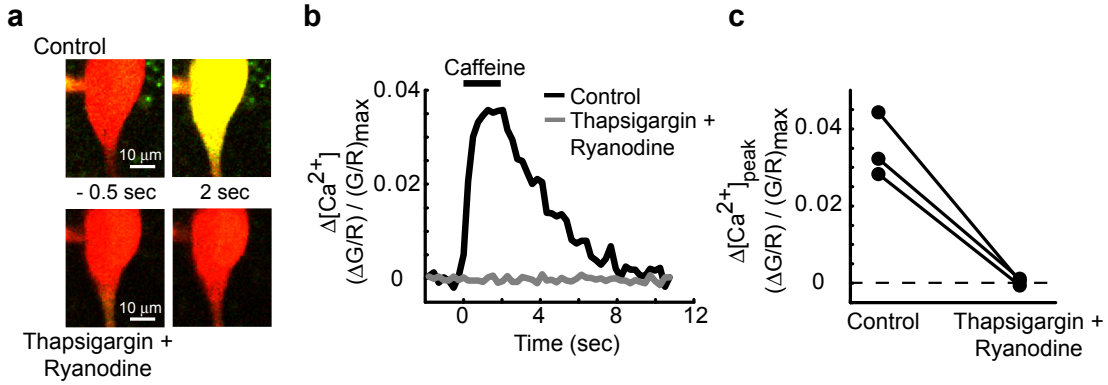

Supplementary Figure 3 | Control for thapsigargin and ryanodine function. a, Example [Ca^{2+}] images before and after caffeine application in the presence or absence of 1 µM thapsigargin and 20 µM ryanodine. The cell was filled with a red (R) Ca^{2+}-insensitive dye (30 µM Alexa 594) and a green (G) Ca^{2+}-sensitive indicator (500 µM Fluo 4FF). At time = 0, caffeine (40 mM) was pressure applied onto the soma for 2 seconds. **b,** Caffeine-induced [Ca^{2+}] transients for the example shown in (a). **c,** Peak caffeine-induced [Ca^{2+}] accumulations before and after application of thapsigargin and ryanodine. n = 3, $p < 0.01$.

Supplementary Figure 4

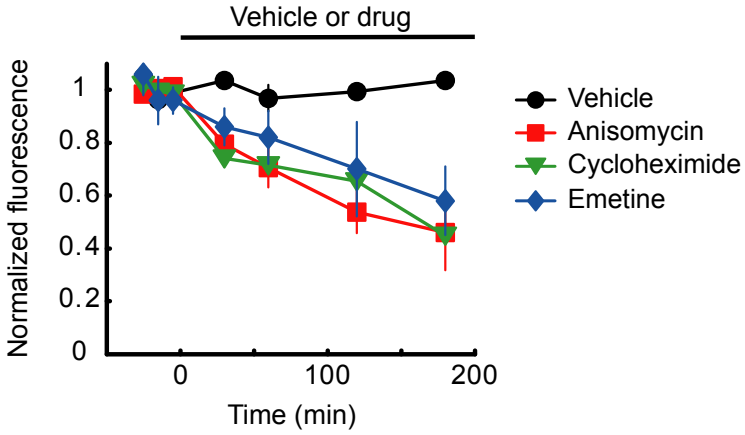

Supplementary Figure 4 | Control for protein synthesis inhibitor function. Time-course of the normalized fluorescence intensity of destabilized EGFP in the thick apical dendrite in the presence of vehicle (0.1% DMSO), 25 µM anisomycin, 60 µM cycloheximide, and 50 µM emetine. For each condition, n = 2, mean ± sem